An Improved Double-Surface Sliding Mode Observer for Flux and Speed Estimation of Induction Motors

S. A. Mansouri [1], A. Ahmarinejad [1], M. S. Javadi [2*], R. Heidari [3], J. P. S. Catalao [2, 4]

[1] Department of Electrical Engineering, Yadegar-e-Imam Khomeini (RAH) Shahre Rey Branch, Islamic Azad University, Tehran, Iran
[2] Institute for Systems and Computer Engineering, Technology and Science (INESC TEC), Porto, Portugal
[3] Department of Electrical Engineering, Shahrekord University, Shahrekord, Iran
[4] Faculty of Engineering of the University of Porto, Porto, Portugal
[*]Corresponding Author: msjavadi@gmail.com

Abstract: This paper studies a double-surface sliding mode observer (DS-SMO) for estimating the flux and speed of induction motors. The sliding mode observer (SMO) equations are based on an induction motor (IM) model in the stationary reference frame. The DS-SMO is developed based on the equations of a single-surface sliding mode observer (SS-SMO) of induction motor. In DS-SMO method, the observer is designed through combining sliding variables produced by combining estimated fluxes of currents error. The speed is easily determined based on the pass of switching signal through a low-pass filter. In addition, an optimal double-surface sliding mode observer (ODS-SMO) is proposed to improve the transient condition by optimally tuning the observer parameters. In order to optimize these parameters, the particle swarm optimization (PSO) method is adopted. Moreover, an improved double-surface sliding mode observer (IDS-SMO) is proposed to improve both transient and steady-state conditions, torque ripple and total harmonic distortion (THD). Moreover, the proposed IDS-SMO has a stable performance under sudden load change and low speed region. Finally, the accuracy of proposed ODS-SMO and IDS-SMO methods is substantiated through simulation and experimental results.

1. Introduction

The induction motor plays a major role in different industrial processes, particularly in electrical pumps, compressors and fans, as well as high-performance applications such as hybrid electric vehicles. Unlike slip ring induction motor, squirrel cage induction motor is very strong, offers a wide torque-speed range, and requires no maintenance. In applications required precise speed or torque control, the IM is usually supplied by a three-phase inverter and controlled through the field orientation control (FOC) method. The FOC enables high-performance drive; therefore, it is preferred to scalar control methods like V/Hz. The rotor field orientation is the most common method of vector control of IMs, since this method decouples d- and q-axis current components at the steady-state situation (not transient situation); hence, the currents could easily follow their command values. In fact, the use of current control method based on proportional-integral (PI) controllers with or without the use of dynamic decoupling terms is prevalent [1-9].

In rotor field-oriented control, the rotor flux angle is required. This angle can be determined through direct field orientation (DFO) or indirect field orientation (IFO) methods. The IFO method is based on the integration of the equation of motor slip in the synchronous reference frame. The rotor flux angle determined through this method is sensitive to the rotor resistance value. In DFO method, the flux angle is determined through inverse tangent of β-axis rotor flux to α-axis rotor flux. The α and β rotor fluxes are usually estimated through an observer. These observers are determined through linear, non-linear or sliding mode methods and estimate state variables.

Combining estimation with adaptation [4, 5, 8, 9, 11], estimating the parameters [25, 29], and performing through non-continuous feedback terms and sliding mode movement on one or multiple sliding variables [13-20], [22-26], [29-32] are various classifications of observer-based methods. Among these methods, the sliding mode observer (SMO) method has the benefit of resisting against uncertainties and providing order reduction.

The n-dimension equations of state space are considered as

$$\begin{cases} \dot{x} = Ax + Bu \\ y = Cx \end{cases} \quad (1)$$

If the supposed m-dimensional state vector x is measurable and matrices A, B and C are time-invariant, design of SMO is straightforward. By adopting the general method detailed in [13], the designed observer has m sliding variables, and the movement of sliding mode is applied to the intersection of sliding variables.

The measured stator currents of IM are among state variables of the system. Therefore, current errors are commonly considered as sliding variables of the observer.

In general, the state space system of IM is time-variant since the speed term emerges in matrix A; hence, sliding mode design cannot be directly utilized. In addition, for sensor-less application, the estimation of speed is required.

In the sensor-less control of IM, the speed, rotor flux magnitude and angle must be estimated. From a theoretical viewpoint, if parameters of the motor are definite, several

methods can be adopted for determining these variables; however, from the practical point of view, there are two problems to be raised here. First, how could one trust the estimations while IM parameters vary with the operating point (i.e. temperature, saturation and the skin effect)? Second, how can the algorithms operate well in real implementation and wide speed range, especially on a digital signal processor with limited accuracy when some estimators adopt complicated or practically untrustworthy methods?

In general, model-dependent estimation methods require precise knowledge of system parameters. In IMs, the magnetizing inductance depends on the flux and saturates in high loads, and stator and rotor resistance are temperature-dependent. In order to improve the estimation accuracy, the temperature of the stator can be measured through thermocouple. Then, the new value of R_s is used in the algorithm. The magnetizing inductance can approximately vary with various operating conditions.

In [29], a second-order function of Lm is given as a function of id. However, the coefficients of this second-order equation must be determined in practice for a given motor.

Concurrent estimation of flux, speed and rotor time constant through sliding mode methods and presupposition of slow changes of speed and rotor time constant is presented in [20, 25]. Under similar presumptions and while knowing the flux, the model-reference adaptive system (MRAS) can estimate speed [30, 31]. The practical accuracy of these methods depends on the quality of laboratory devices, ability to operate under pulse-width modulation (PWM) noise, and DC off-set conditions.

In [20] – [22], the observer determines the flux of rotor by the integration of an equivalent control signal. In this method, estimation of flux requires a precise value of L_m. Unlike [21] and [22], [20] presents a method insensitive to the rotor resistance.

In [23], a sliding mode observer for the flux magnitude of the IM is analysed by using a modified model of the motor in the rotating reference frame. In this method, despite estimating inaccurate speed, a precise flux is attained by designing of the feedback gains.

A nonlinear control based on combining the conventional PI control with a high-order fast terminal sliding mode (HOFTSM) load torque observer is proposed in [24]. In this method, the estimated torque is utilized as a feed-forward compensation for the PI controller to enhance the performance of motor under sudden load changes. In [17], three sensor-less sliding mode observers and their parameter sensitivity analysis are presented, and their accuracy depended on the values of L_m and R_r is investigated.

A successive estimation method is suggested in [26, 27]. In this method, speed is initially estimated, and the estimated speed is used in the SMO to estimate the flux of rotor.

Speed control at zero and very low frequencies is increasingly studied in new research [34, 35]. In [34], an adaptive sliding mode observer is designed to estimate the stator current, rotor flux, and rotor speed. In addition, a Lyapunov function based on the rotor fluxes error and speed estimation error is utilized to improve the performance of motor at low speed and standstill operation. A direct field oriented control is applied to space vector pulse Width modulation based on SMO to estimate the speed and flux at low speed precisely.

In this paper, the double-surface sliding mode observer in [15] is developed by utilizing particle swarm optimization (PSO) algorithm. In the proposed IDS-SMO, the control parameters are estimated by PSO algorithm. The proposed ODS-SMO has faster dynamic speed response while making the steady-state condition worse compared to the DS-SMO [15]. In addition, to improve both transient and steady-state performance and reduce torque ripple and current harmonics, an improved double-surface sliding mode observer (IDS-SMO) is proposed. The proposed IDS-SMO has also great performance under sudden load change compared to the proposed ODS-SMO and DS-SMO [15].

In the second section of this paper, the equations of IM state space are developed by considering the fluxes and the stator currents as state-variables in the stationary reference frame. Then, equations related to the double-surface sliding mode observer, extended based on a single-surface sliding mode observer [15], are introduced. Next, particle swarm optimization algorithm and an improved double-surface sliding mode observer is introduced. Later, the proposed ODS-SMO, IDS-SMO and DS-SMO [15] methods are simulated and compared. The experimental results are finally presented to support the effectiveness of proposed IDS-SMO in terms of precise speed estimation, the rotor flux magnitude estimation, and the torque ripple reduction.

2. Induction motor model

The state-space model of induction motor in the stationary reference frame [13] is

$$\begin{cases} \dfrac{d\lambda_{r\alpha}}{dt} = -\eta\lambda_{r\alpha} - \omega_r\lambda_{r\beta} + \eta L_m i_{s\alpha} \\ \dfrac{d\lambda_{r\beta}}{dt} = \omega_r\lambda_{r\alpha} - \eta\lambda_{r\beta} + \eta L_m i_{s\beta} \\ \dfrac{di_{s\alpha}}{dt} = \eta\beta\lambda_{r\alpha} + \omega_r\beta\lambda_{r\beta} - \gamma i_{s\alpha} + \dfrac{1}{\sigma L_s} v_{s\alpha} \\ \dfrac{di_{s\beta}}{dt} = -\omega_r\beta\lambda_{r\alpha} + \eta\beta\lambda_{r\beta} - \gamma i_{s\beta} + \dfrac{1}{\sigma L_s} v_{s\beta} \end{cases} \quad (2)$$

where $\lambda_{r\alpha}$ and $\lambda_{r\beta}$ are the rotor fluxes, and $i_{s\alpha}$, $i_{s\beta}$, $v_{s\alpha}$ and $v_{s\beta}$ are the stator currents and voltages all in the stationary reference frame. In addition, L_s and L_m represent the stator and magnetising inductances, and ω_r refers to the electrical speed of rotor, which is related to the mechanical speed as: $\omega_r = n_p * \omega_{mech}$. The parameters σ, β, γ and η are determined through following equations.

$$\begin{aligned} \sigma &= 1 - \frac{L_m^2}{L_s L_r}. & \beta &= \frac{L_m}{\sigma L_s L_r} \\ \eta &= \frac{R_r}{L_r}. & \gamma &= \frac{1}{\sigma L_s}\left(\frac{L_m^2}{L_r^2} R_r + R_s\right) \end{aligned} \quad (3)$$

3. Field-Oriented Control

Field-oriented control (FOC) technique is being utilized extensively for the control of induction motors. This technique allows the squirrel cage induction motor to be driven with high performance comparable to that of a DC motor. The principle of FOC is to keep a suitable alignment between the stator and rotor flux [36].

3.1. Direct Field Oriented Control

In the direct field oriented control (DFOC), the rotor flux angle is estimated by an observer or measured by flux sensor. The rotor flux cannot be directly measured by sensors. In fact, through direct measuring of signal, it is possible to calculate the rotor flux, which might cause errors at low speed.

3.2. Rotor Field-Oriented Control

The main principle of field-oriented control of IMs is that the d-axis are aligned with the rotor flux vector. Therefore, this leads to decouple of target variables so that the flux and torque can be independently controlled by d- and q-axis stator current components, respectively.

The voltage equation of IM in the d-q reference frame is:

$$\begin{aligned} V_{qs} &= R_s i_{qs} + \omega\lambda_{ds} + \frac{d\lambda_{qs}}{dt} \\ V_{ds} &= R_s i_{ds} + \omega\lambda_{qs} + \frac{d\lambda_{ds}}{dt} \\ 0 &= R_r i_{qr} + (\omega - \omega_r)\lambda_{dr} + \frac{d\lambda_{qr}}{dt} \\ 0 &= R_r i_{dr} + (\omega - \omega_r)\lambda_{qr} + \frac{d\lambda_{dr}}{dt} \end{aligned} \tag{4}$$

Where the stator and rotor flux can be estimated by following

$$\begin{aligned} \lambda_{qs} &= L_s i_{qs} + L_m i_{qr} \\ \lambda_{ds} &= L_s i_{ds} + L_m i_{dr} \\ \lambda_{qr} &= L_r i_{qr} + L_m i_{qs} \\ \lambda_{dr} &= L_r i_{dr} + L_m i_{ds} \end{aligned} \tag{5}$$

The electromagnetic torque is calculated by (6)

$$T_e = \frac{3n_p}{2}\frac{L_m}{L_r}\left(\lambda_{dr} i_{qs} - \lambda_{qr} i_{ds}\right) \xrightarrow{\lambda_{qr}=0} T_e = \frac{3n_p}{2}\frac{L_m}{L_r}\lambda_{dr} i_{qs} \tag{6}$$

In order to estimate the rotor flux angle, the stator flux is first estimated in the stationary reference frame through

$$\begin{aligned} \lambda_{s\alpha} &= \int (v_{s\alpha} - R_s i_{s\alpha})dt \\ \lambda_{s\beta} &= \int (v_{s\beta} - R_s i_{s\beta})dt \end{aligned} \tag{7}$$

And the rotor flux is then calculated by following manner

$$\begin{aligned} \lambda_{r\alpha} &= \frac{L_r}{L_m}(\lambda_{s\alpha} - \sigma L_s i_{s\alpha}) \\ \lambda_{r\beta} &= \frac{L_r}{L_m}(\lambda_{s\beta} - \sigma L_s i_{s\beta}) \end{aligned} \tag{8}$$

Then the rotor flux angle is obtained by (9).

$$\theta_{\lambda r} = \tan^{-1}\left(\frac{\lambda_{r\beta}}{\lambda_{r\alpha}}\right) \tag{9}$$

Consequently, the motor variables such as voltages and currents must be transformed to this reference frame.

$$f_{dqs} = f_{ds} + j f_{qs} = f_{abcs} e^{-j\theta_{\lambda r}} \qquad f \in \{v, i\} \tag{10}$$

Since the rotor flux is aligned with d-axis

$$\lambda_{qr} = 0 \;\rightarrow\; 0 = R_r i_{dr} + \frac{d\lambda_{dr}}{dt} \tag{11}$$

In addition, as the rotor current is not measurable, therefore the i_{dr} must be removed from (11) as following

$$\lambda_{dr} = L_m i_{ds} - \frac{L_r}{R_r}\frac{d\lambda_{dr}}{dt} \;\rightarrow\; \lambda_{dr} = \frac{L_m}{1 + \frac{d}{dt}(\frac{L_r}{R_r})} i_{ds} \tag{12}$$

Based on (12), the rotor flux can be controlled by i_{ds}, and the electromagnetic torque can be controlled by i_{qs} if the rotor flux is kept constant. Fig. 1 depicts the overall block diagram of RFOC.

4. Proposed Optimal Double-Surface Observer for Speed and Flux Estimation of Induction Motor

In this paper, the DS-SMO method are optimized by utilizing PSO algorithm. The PSO is employed in order to achieve faster dynamic response of speed and torque.

4.1. Double-Surface Observer for Speed and Flux Estimation of Induction Motor

The double-surface sliding mode observer is developed by adding additional feedback terms to the single-surface sliding mode observer [13, 32]. In [15], it is practically and analytically shown that SS-SMO becomes convergent in distinct conditions. The sliding variables of a DS-SMO are selected in the following manner.

$$\begin{cases} s_1 = \hat{\lambda}_{r\alpha}\bar{\imath}_{s\beta} - \hat{\lambda}_{r\beta}\bar{\imath}_{s\alpha} \\ s_2 = \hat{\lambda}_{r\alpha}\bar{\imath}_{s\alpha} + \hat{\lambda}_{r\beta}\bar{\imath}_{s\beta} \end{cases} \tag{13}$$

where $\hat{\lambda}_{r\alpha}$ and $\hat{\lambda}_{r\beta}$ refer to the estimated rotor fluxes while $\bar{\imath}_{s\alpha} = \hat{\imath}_{s\alpha} - i_{s\alpha}$ and $\bar{\imath}_{s\beta} = \hat{\imath}_{s\beta} - i_{s\beta}$ signify error of real and estimated stator currents. If the movement of sliding mode attains such surfaces, we have $s_1 = 0$ and $s_2 = 0$. This is equivalent with:

$$\begin{bmatrix} -\hat{\lambda}_{r\beta} & \hat{\lambda}_{r\alpha} \\ \hat{\lambda}_{r\alpha} & \hat{\lambda}_{r\beta} \end{bmatrix} \begin{bmatrix} \bar{\imath}_{s\alpha} \\ \bar{\imath}_{s\beta} \end{bmatrix} = \begin{bmatrix} 0 \\ 0 \end{bmatrix} \tag{14}$$

As $\det(\Lambda) = -(\hat{\lambda}_{r\alpha}^2 + \hat{\lambda}_{r\beta}^2) \neq 0$, (14) has a unique solution (i.e. $\bar{\imath}_{s\alpha} = 0$ and $\bar{\imath}_{s\beta} = 0$). Therefore, the convergence of currents estimation of this observer will be provided. The equations for DS-SMO are as represented in the following.

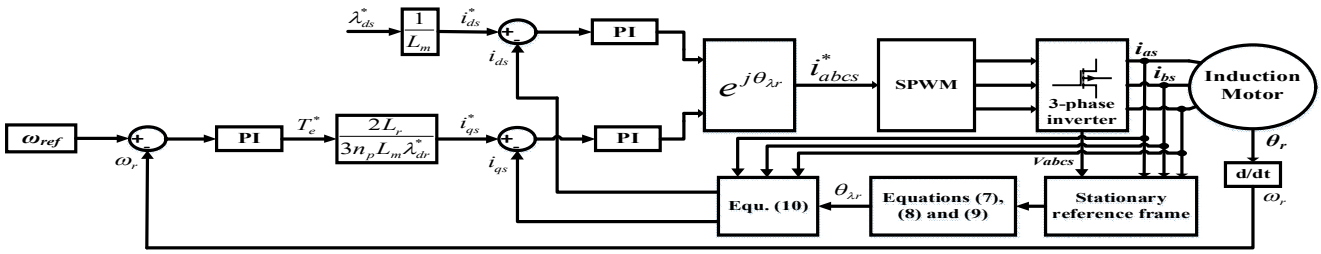

Fig. 1. *Overall block diagram of rotor field oriented control of induction motor*

$$\begin{cases} \dfrac{d\hat{\lambda}_{r\alpha}}{dt} = -\eta\hat{\lambda}_{r\alpha} - \hat{\omega}_r\hat{\lambda}_{r\beta} + \eta L_m i_{s\alpha} \\ \dfrac{d\hat{\lambda}_{r\beta}}{dt} = \hat{\omega}_r\hat{\lambda}_{r\alpha} - \eta\hat{\lambda}_{r\beta} + \eta L_m i_{s\beta} \\ \dfrac{d\hat{\imath}_{s\alpha}}{dt} = \eta\beta\hat{\lambda}_{r\alpha} + \hat{\omega}_r\beta\hat{\lambda}_{r\beta} - \gamma i_{s\alpha} + \dfrac{1}{\sigma L_s}v_{s\alpha} - k\hat{\lambda}_{r\alpha}u_2 \\ \dfrac{d\hat{\imath}_{s\beta}}{dt} = -\hat{\omega}_r\beta\hat{\lambda}_{r\alpha} + \eta\beta\hat{\lambda}_{r\beta} - \gamma i_{s\beta} + \dfrac{1}{\sigma L_s}v_{s\beta} - k\hat{\lambda}_{r\beta}u_2 \end{cases} \quad (15)$$

Where k is a design parameter. If it is equal to zero, it will signify a SS-SMO [13]. The switching terms are:

$$\begin{cases} \hat{\omega}_r = \omega_0.sign(s_1) \\ u_2 = M.sign(s_2) \end{cases} \quad (16)$$

Here, ω_0 and M refer to design gains. After subtraction, the error of estimations is equal with:

$$\begin{cases} \dfrac{d\bar{\lambda}_{r\alpha}}{dt} = -\eta\bar{\lambda}_{r\alpha} - \hat{\omega}_r\hat{\lambda}_{r\beta} + \omega_r\lambda_{r\beta} \\ \dfrac{d\bar{\lambda}_{r\beta}}{dt} = \hat{\omega}_r\bar{\lambda}_{r\alpha} - \omega_r\lambda_{r\alpha} - \eta\bar{\lambda}_{r\beta} \\ \dfrac{d\bar{\imath}_{s\alpha}}{dt} = \eta\beta\bar{\lambda}_{r\alpha} + \hat{\omega}_r\beta\hat{\lambda}_{r\beta} - \omega_r\beta\lambda_{r\beta} - k\hat{\lambda}_{r\alpha}u_2 \\ \dfrac{d\bar{\imath}_{s\beta}}{dt} = -\hat{\omega}_r\beta\hat{\lambda}_{r\alpha} + \omega_r\beta\lambda_{r\alpha} + \eta\beta\bar{\lambda}_{r\beta} - k\hat{\lambda}_{r\beta}u_2 \end{cases} \quad (17)$$

In order to review the occurrence of sliding mode, the two sliding variables are derived, and derivatives are substituted. The derivative of S_1 is:

$$\begin{aligned} \dot{s}_1 = &-\eta\left(\hat{\lambda}_{r\alpha}\bar{\imath}_{s\beta} - \hat{\lambda}_{r\beta}\bar{\imath}_{s\alpha}\right) - \hat{\omega}_r\left(\hat{\lambda}_{r\alpha}\bar{\imath}_{s\alpha} + \hat{\lambda}_{r\beta}\bar{\imath}_{s\beta}\right) \\ &+\eta L_m\left(i_{s\alpha}\bar{\imath}_{s\beta} + i_{s\beta}\bar{\imath}_{s\alpha}\right) + \beta\omega_r\left(\hat{\lambda}_{r\alpha}\lambda_{r\alpha} + \hat{\lambda}_{r\beta}\lambda_{r\beta}\right) \\ &+\beta\eta\left(\bar{\lambda}_{r\beta}\hat{\lambda}_{r\alpha} - \bar{\lambda}_{r\alpha}\hat{\lambda}_{r\beta}\right) - \beta\hat{\omega}_r\left(\hat{\lambda}_{r\alpha}^2 + \hat{\lambda}_{r\beta}^2\right) \end{aligned} \quad (18)$$

and the derivative of S_2 is equal with:

$$\begin{aligned} \dot{s}_2 = &-\eta\left(\hat{\lambda}_{r\alpha}\bar{\imath}_{s\alpha} - \hat{\lambda}_{r\beta}\bar{\imath}_{s\beta}\right) + \hat{\omega}_r\left(\hat{\lambda}_{r\alpha}\bar{\imath}_{s\beta} - \hat{\lambda}_{r\beta}\bar{\imath}_{s\alpha}\right) \\ &+\eta L_m\left(i_{s\alpha}\bar{\imath}_{s\alpha} + i_{s\beta}\bar{\imath}_{s\beta}\right) + \beta\eta\left(\bar{\lambda}_{r\alpha}\hat{\lambda}_{r\alpha} + \bar{\lambda}_{r\beta}\hat{\lambda}_{r\beta}\right) \\ &-\beta\omega_r\left(\hat{\lambda}_{r\alpha}\lambda_{r\beta} - \hat{\lambda}_{r\beta}\lambda_{r\alpha}\right) - k\left(\hat{\lambda}_{r\alpha}^2 + \hat{\lambda}_{r\beta}^2\right)u_2 \end{aligned} \quad (19)$$

It should be noted that the switching term u_2 has not emerged in (18). The equations (18) and (19) can be rewritten in the following manner.

$$\begin{cases} \dot{s}_1 = f_1 - \beta\left(\hat{\lambda}_{r\alpha}^2 + \hat{\lambda}_{r\beta}^2\right).\omega_0.sign(s_1) \\ \dot{s}_2 = f_2 - k\left(\hat{\lambda}_{r\alpha}^2 + \hat{\lambda}_{r\beta}^2\right).M.sign(s_2) \end{cases} \quad (20)$$

The functions f_1 and f_2 include estimations, error of estimations as well as speed and motor parameters. If estimations are limited, both functions will have a top-limit, and they will not tend to indefinite. Based on (20), if gains ω_0 and M are selected as sufficiently large while $\hat{\lambda}_{r\alpha}^2 + \hat{\lambda}_{r\beta}^2 \neq 0$ is presumed, the switching terms at the right side of (20) will be as shown in the following.

$$\begin{cases} \beta\left(\hat{\lambda}_{r\alpha}^2 + \hat{\lambda}_{r\beta}^2\right).\omega_0 > |f_1| \\ k\left(\hat{\lambda}_{r\alpha}^2 + \hat{\lambda}_{r\beta}^2\right).M > |f_2| \end{cases} \quad (21)$$

Therefore, S_1 and $\dot{S}_1$ as well as S_2 and $\dot{S}_2$ will have opposite signs. As a result, sliding variables are attractive, and $s_1 \to 0$ and $s_2 \to 0$. Hence, sliding mode occurs at the intersections of these variables. Because ω_0 and M are sole gains of observer design (gain k can be presumed at M), the only condition that should be satisfied is (21). In order to satisfy the condition, it is necessary to determine the maximum values of functions f_1 and f_2 for proper design of gains.

Employing s_1 along sliding mode, because $\bar{\imath}_{s\alpha} = 0$ and $\bar{\imath}_{s\beta} = 0$, it results in $\left(\hat{\lambda}_{r\alpha}\bar{\imath}_{s\alpha} - \hat{\lambda}_{r\beta}\bar{\imath}_{s\beta}\right) = 0$. Consequently, only one term is dependent on $\hat{\omega}_r$ in (18). With the assumption that $s_1 = 0$ and $\dot{s}_1 = 0$, the equivalent control signal is determined as follows.

$$\omega_{r.eq} = \omega_r\frac{\lambda_{r\alpha}\hat{\lambda}_{r\alpha} + \lambda_{r\beta}\hat{\lambda}_{r\beta}}{\hat{\lambda}_r^2} + \eta\frac{\hat{\lambda}_{r\alpha}\bar{\lambda}_{r\beta} - \hat{\lambda}_{r\beta}\bar{\lambda}_{r\alpha}}{\hat{\lambda}_r^2} \quad (22)$$

Because the fluxes become convergent, the second term in (22) is zero, while other terms are 1. Therefore, it is obvious that $\omega_{r.eq} \to \omega_r$. The estimated speed tends toward the actual speed with a rate that depends on "reduction rate of sliding variable" or "S_1". If $\bar{\lambda}_{r\alpha}$ and $\bar{\lambda}_{r\beta}$ are always zero, and the movement of sliding mode on S_1 is not disturbed, $\omega_{r.eq}$ is precisely equal to ω_r. In this method, speed estimation can be obtained through passing the sliding variable s_1 through a low-pass filter. As a result, time constant of filter, τ_f, can be affected estimation of speed, and it must be optimally selected. Based on (21), design of ω_0 requires $\beta\left(\hat{\lambda}_{r\alpha}^2 + \hat{\lambda}_{r\beta}^2\right)\cdot\omega_0 > |f_1|$. Thus, for a drive operating at the variable flux surfaces and variable speed (f_1 is dependent on speed), a proper value can be acquired for ω_0. Another essential condition is $\omega_0 > \omega_r$ since speed estimation is obtained through filtering of switching term $\omega_0 \cdot sign(s_1)$. If motor is required to operate at low-speed region, the high value of ω_0 can be problematic (development of chattering phenomenon).

It should be also noted that movement of sliding mode on the surface s_1 is independent of the switching term $M\cdot$

$sign(s_2)$. However, the movement of s_2 includes the term $\omega_0 \cdot sign(s_1)$, and when the observer operates under unsuitable parameters, the term can operate as a disturbance. Therefore, value of ω_0 must not exceed the design limit (for instance, if drive operates at 300 rad/s, it is harmful to utilize a value of ω_0 higher than 1.5-2 times of 300 rad/s [15]). Figs. 2 and 3 depict the effect of deign gains and time constant of low-pass filter on the accuracy of motor speed estimation and transient-state response.

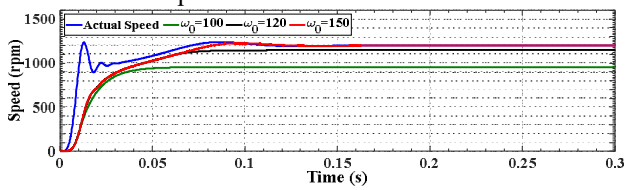

Fig. 2. *Effect of ω_0 on speed estimation*

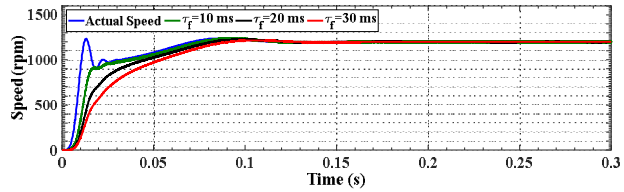

Fig. 3. *Effect of τ_f on speed estimation*

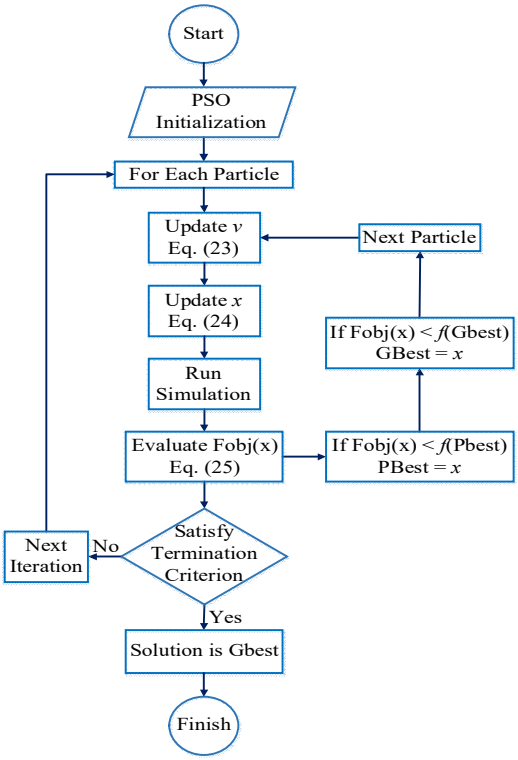

Fig. 4. *Flowchart of PSO algorithm*

4.2. Particle Swarm Optimization

The particle swarm optimization technique is first introduced by Kennedy and Eberhart in 1995 [33]. The main purpose of this algorithm was simulating collective behaviour of bird flock or fish school. Based on improving and changing animal Behaviour Model, a strong optimization method is proposed. Although this method is first introduced to optimize nonlinear continuous problems, much progress is performed to improve and use this algorithm to optimize complex problems in different branches of engineering.

The PSO algorithm is a population-based evolutionary technique. It has important features compared to other optimization methods:

- Unlike many common methods, this algorithm does not require a derivative of the objective function.
- It can be combined with other optimization methods.
- It has less sensitive to cost function.
- Unlike many other evolutionary approaches, it has fewer regulatory parameters.
- It is easy to implement with simple mathematical relationships and logical operators.

Simplicity is the main feature of the PSO algorithm. In fact, this method can be implement with merely two equations. In this method, speed and location of each particle in searching process are determined through (23) and (24), respectively.

$$v_i^{k+1} = v_i^k + c_1 r_1 (Pbest_i - x_i^k) + c_2 r_2 (Gbest - x_i^k) \quad (23)$$

$$x_i^{k+1} = x_i^k + v_i^{k+1} \quad (24)$$

Where c_1 and c_2 are two constant numbers to determine the computation time and the number of iteration, r_1 and r_2 signify two random numbers, v_i^k refers to speed of ith particle at kth iteration, x_i^k refers to location of ith particle at kth iteration, $Pbest_i$ is the best solution of ith particle, and Gbest signifies the best solution of all particles. The PSO algorithm process is as following:

1- Production of the initial population
2- Start the main loop
3- Update the speed of *i*th particle
4- Update the place of *i*th particle
5- Evaluation of objective function
6- Update Pbest for *i*th particle
7- Update Gbest
8- If all particles are not evaluated, and the end condition of the main loop is not finished, put i=i+1 and go to level 3.
9- If all particles are evaluated, and the end condition of the main loop is not finished, put i=1 and go to level 2.
10- If the end condition of the main loop is finished, go to level 11.
11- Plot the result

The process of implementing this algorithm is represented in Fig. 4.

4.3. Objective Function

In this paper, the main objective is the optimization of DS-SMO by considering the parameters ω_0, M and time constant of low-pass filter (τ_f) as optimization variables so that the convergence speed and accuracy of estimation are attained. Hence, the objective function can be represented as:

$$F_{obj} = \int_0^T t(|e_\omega| + |e_\lambda|)dt \quad (25)$$

Where T refers to the total simulation time, e_ω refers to speed estimation error, and e_λ represents flux estimation error.

5. Proposed Improved Double-Surface Sliding Mode Observer

Although the proposed ODS-SMO has better dynamic speed response compared to the DS-SMO method, the steady-state condition includes severe current harmonic and torque ripple. In order to address this poor performance during steady-state condition, an improved double-surface sliding mode observer is introduced. In this method, the sign function is substituted by saturation function and the low-pass filter (LPF) is removed. In fact, the saturation function removes chattering effect result in better steady-state performance, and removing LPF can improve transient condition and remove delay.

$$\begin{cases} \hat{\omega}_r = \omega_0 . sat(s_1) \\ u_2 = M . sat(s_2) \end{cases} \quad (26)$$

It is significant to be mentioned that the parameters ω_0 and M are optimally determined by PSO algorithm.

The values of sliding mode observer for all studied methods are represented in Table 1. The values of ODS-SMO and IDS-SMO have been selected by PSO method. The parameters of motor are also represented in Table 2.

Table 1 Different values of sliding mode observer

Method	ω_0	M	τ_f
DS-SMO [15]	400	40	0.0667
ODS-SMO	386.7712	9.1599	0.0012
IDS-SMO	995.5	99.549	LPF is removed

Table 2 Parameters of induction motor

P	ω_n	T_n	L_m	L_{lr}	L_{ls}	R_r	R_s
4	1390 rpm	4 N.m	0.30 H	0.015 H	0.015 H	5.57 Ω	10.9 Ω

6. Simulation Results

In order to conduct the comparison, simulation was performed with the values mentioned in [15] and proposed ODS-SMO and IDS-SMO (Table 1) in MATLAB/Simulink. The sample-time is set at $10\,\mu s$. The results of speed estimation and fluxes are represented in Figs 5-7.

6.1. Transient-state analysis

As it can be seen from Figs. 5-7 (a), although the proposed ODS-SMO has a faster dynamic speed response compared to DS-SMO, the proposed IDS-SMO can follow the actual speed with the minimum delay in comparison with the other methods. The most significant parameter to decrease delay is removing low-pass filter in the proposed IDS-SMO method.

6.2. Steady-state analysis

Figs. 5-7(b) illustrate the speed error of all methods. As it is expected, decreasing the time constant of low-pass filter can improve the transient response (Fig. 6(a)); however, it makes steady state operation the worst (Fig. 6(b)). By removing the LPF in the proposed IDS-SMO ($\tau_f \to \infty$), the minimum speed error is anticipated in the steady-state performance.

In addition, Figs. 5-7(c) show that the estimated flux follows the actual flux in all methods precisely. Nonetheless, the proposed method has the best accuracy (Fig. 7(d)).

In addition, by optimizing the coefficient in the proposed ODS-SMO, the flux becomes more balanced, and the flux error is decreased compared to the DS-SMO method [15] (Figs. 5(d) and 7(d)).

In order to investigate the response of all methods, another simulation is performed while the motor is run at no-load condition. Then, full-load is applied to the motor at t=5 (sec).

As it can be seen from Figs. 8(a) and (b), the DS-SMO method [15] and the proposed ODS-SMO have unreasonable dynamic speed response. In fact, reset the coefficient is fundamental in this situation to achieve stable performance. However, the response of proposed ODS-SMO is much better compared to DS-SMO [15].

In addition, Fig. 8(c) depicts the stable performance of proposed IDS-SMO without changing the coefficients.

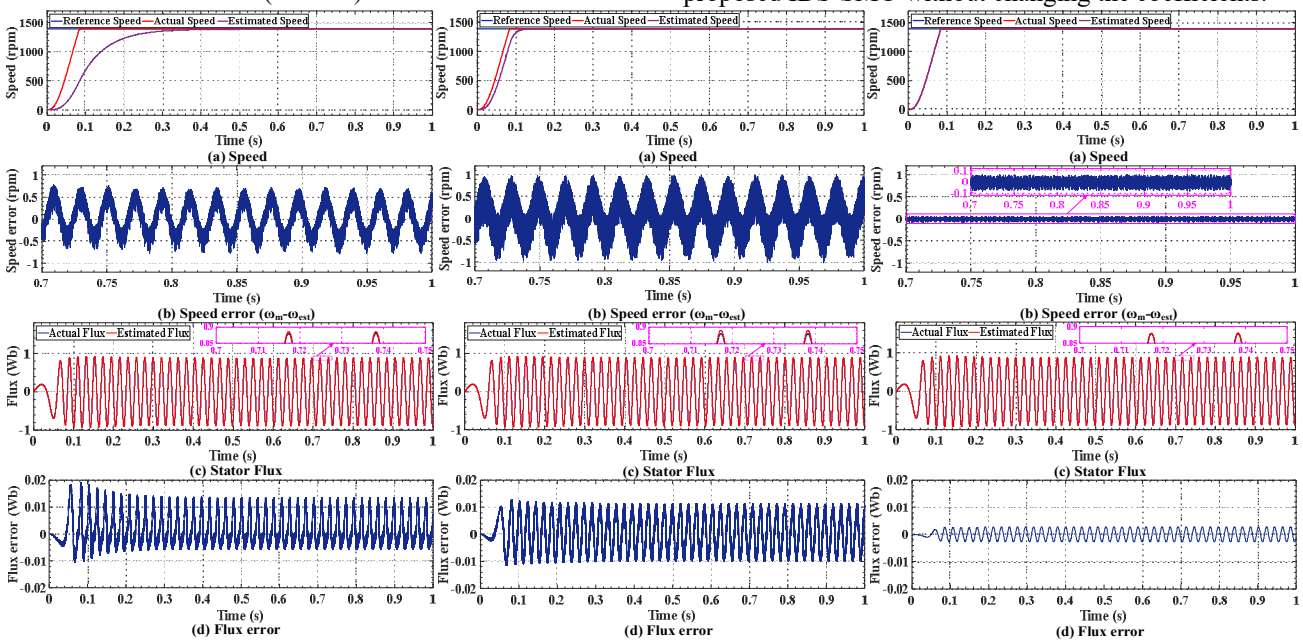

Fig. 5. DS-SMO [15]

Fig. 6. Proposed ODS-SMO

Fig. 7. Proposed IDS-SMO

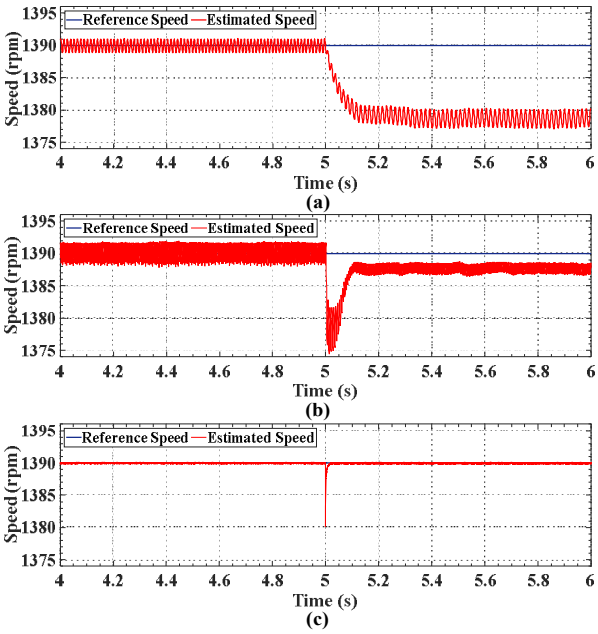

Fig. 8. *Close-loop control with different estimated speed (a) DS-SMO [15], (b) proposed ODS-SMO, and (c) proposed IDS-SMO*

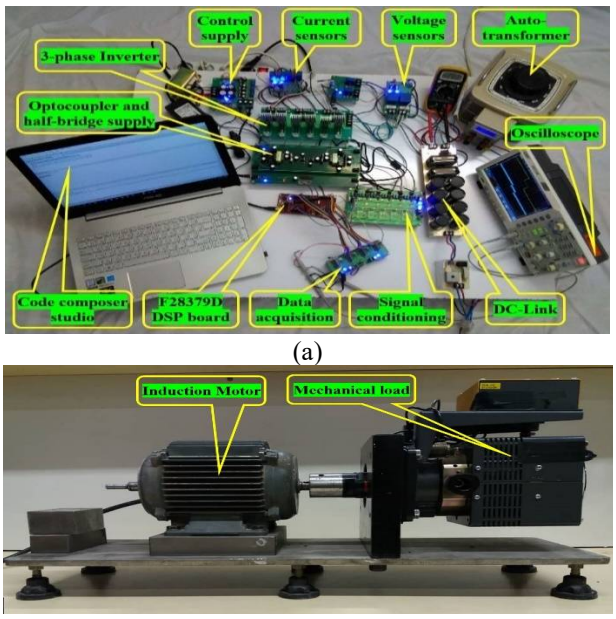

Fig. 9. *The setup used for practical tests*

7. Experimental Results

In order to evaluate the practical effectiveness of the proposed IDS-SMO method, three tests are performed. A LaunchPad XL TMS320F28379D, a floating-point discrete signal processor board, is utilized to perform the analysed methods coded through Simulink/MATLAB. The sample-time is set at 100 μs. The setup used for experimental tests is depicted in Fig. 9.

7.1. Transient and steady state operation

It is significant to be mentioned that the experimental results of all studied methods are depicted at Fig. 10, 11 and 12. These tests are performed under nominal situation. According to Figs. 11(a) and 12(a), both proposed ODS-SMO and IDS-SMO can improve the transient response compared to the DS-SMO [15] (290 (msec)). It is evident that the proposed IDS-SMO has the fastest transient response (85 (msec))

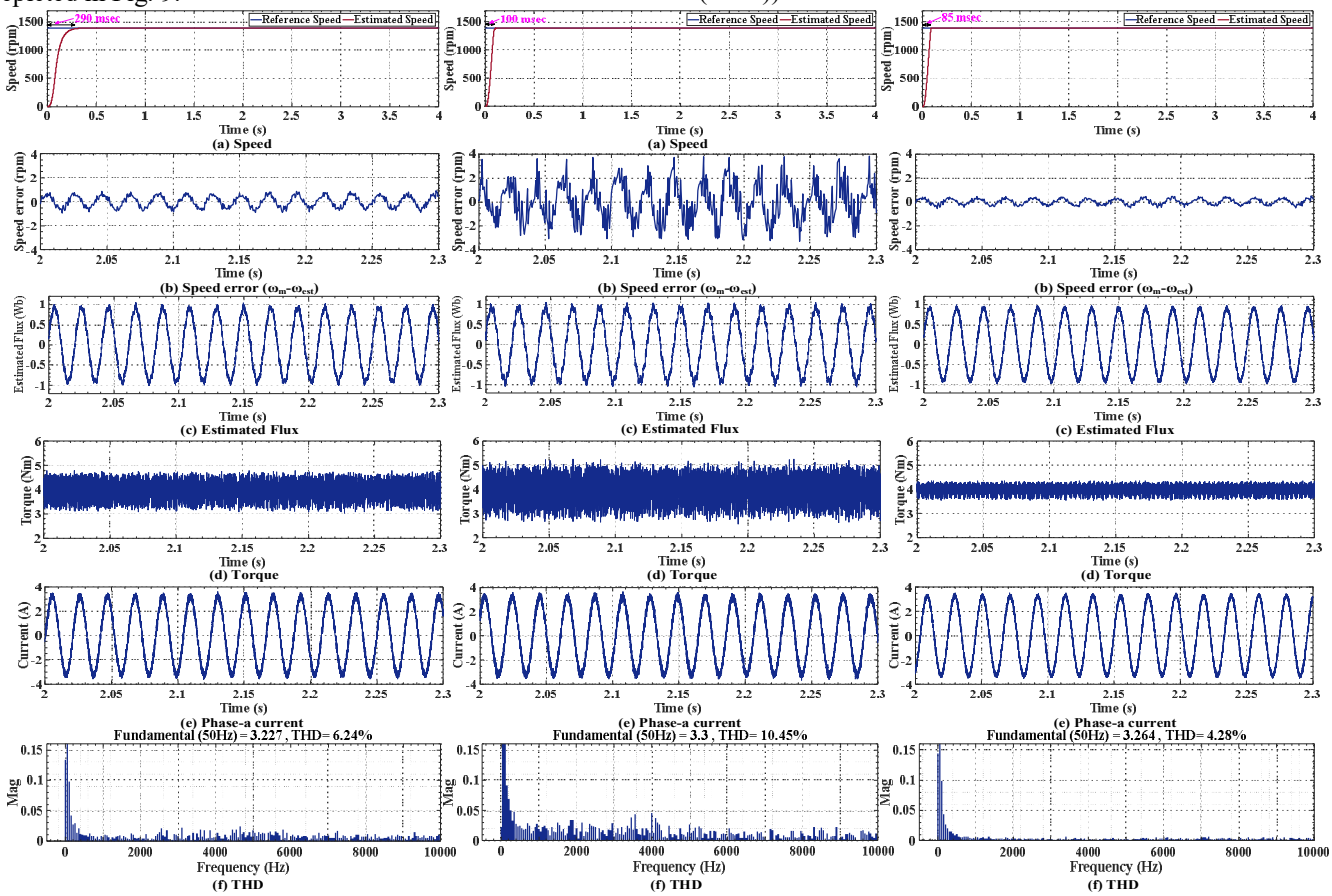

Fig. 10. *DS-SMO [15]*

Fig. 11. *Proposed ODS-SMO*

Fig. 12. *Proposed IDS-SMO*

As it can be seen from Fig. 12, the proposed IDS-SMO has the best performance during steady-state with minimum speed error (Fig. 12(b)), torque ripple (Fig. 12(d)) and total harmonic distortion (Fig. 12(f)). It is also apparent that although the proposed ODS-SMO can improve the transient response, its steady-state performance is the worst one with maximum speed error (Fig. 11(b)), torque ripple (Fig. 11(d)) and total harmonic distortion (Fig. 11(f)).

To evaluate the performance of the proposed IDS-SMO under sudden load-change, another experiment is carried out (Fig. 13). In this test, the nominal load is applied to the motor at t=2(sec) where the motor is run at nominal speed. Figure 13(a) illustrates the estimated speed follows its command precisely before and after employing the nominal load. In addition, the speed and torque response is really fast at about 10 (msec) for speed (Figs. 13(a) and (b)).

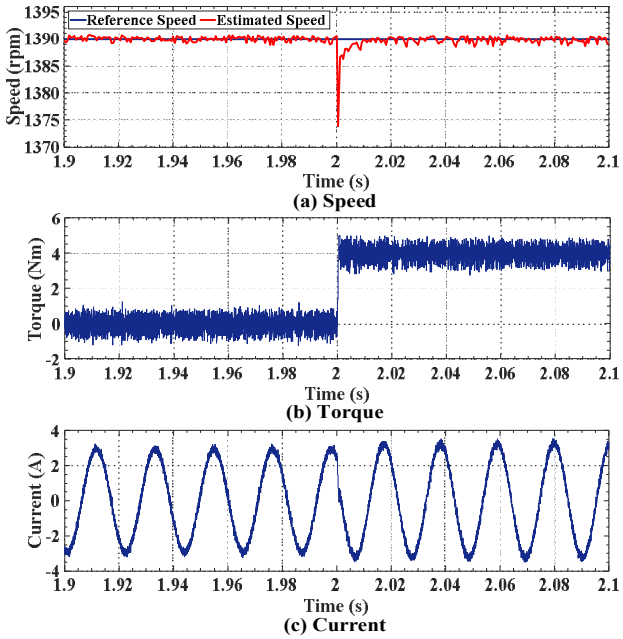

Fig. 13. *Experimental results of proposed IDS-SMO method at nominal situation*

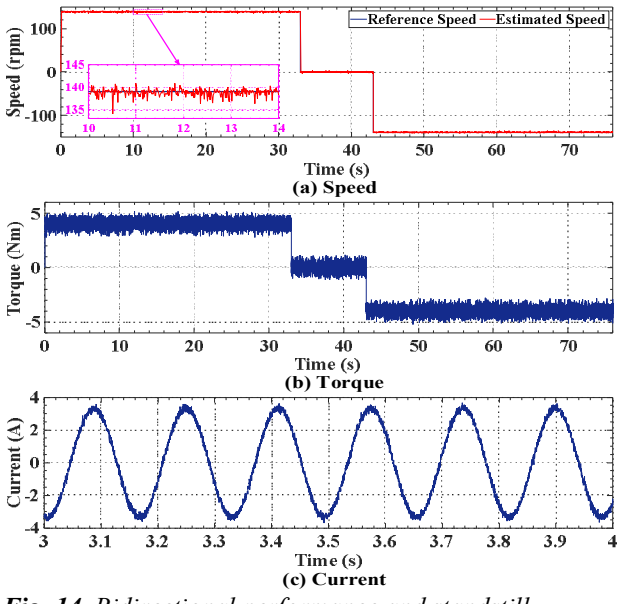

Fig. 14. *Bidirectional performance and standstill operation of proposed IDS-SMO method at low speed region*

7.2. Low speed region and bidirectional operation

The experimental test is also accomplished at low speed region and standstill operation. The speed is set at 10 percent of nominal speed in counter-clockwise direction (139 (rpm)). Then, after a 10-second standstill, the direction is reversed at -139 (rpm) (Fig. 11(a)). Figure 11(b) illustrates that this test is implemented at nominal load. The phase-a current is finally depicted at Fig. 11(c).

8. Conclusion

This paper discusses the problem of speed and flux estimation of an induction motor. In this regard, the double-surface sliding mode observer, extended by adding extra feedback terms to the single-surface sliding mode observer, is studied to enable speed and flux estimation precisely.
In addition, by employing particle swarm optimization algorithm, the optimal double-surface sliding mode observer is proposed to attain faster transient speed response compared to DS-SMO. It is proved that the proposed ODS-SMO is only able to improve the transient response. In addition, it is illustrated that both DS-SMO and proposed ODS-SMO have poor performance when the step-load is applied to the motor. In order to address this problem, the IDS-SMO is proposed. Moreover, the proposed IDS-SMO method improves both the transient and steady-state operations compared to the DS-SMO [15] and proposed ODS-SMO methods. Simulations and experimental studies substantiate that the proposed IDS-SMO method has also a great performance at low speed region and standstill operation.

9. References

[1] Rebah Maamouri, Mohamed Trabelsi, Mohamed Boussak, Faouzi M'Sahli, 'Mixed model-based and signal-based approach for open-switches fault diagnostic in sensorless speed vector controlled induction motor drive using sliding mode observer', IET Power Electron., 2019, vol. 12, no. 5, pp. 1149-1159.

[2] Hinkkanen, M.: 'Analysis and design of full order flux observers for sensorless induction motors', IEEE Trans. Ind. Electron., 2004, 51, (5), pp. 1033–1040.

[3] Mohammad Estahbanati, 'An adaptive control scheme for doubly fed induction generators–wind turbine implementation', Journal of Experimental & Theoretical Artificial Intelligence, 2014, 26, (2), pp. 183-195.

Kim, J.H., Choi, J.W., Sul, S.K., 'Novel rotor flux observer using observer characteristic function in complex vector space for field oriented induction motor drives', IEEE Trans. Ind. Appl., 2002, 38, pp. 1334–1343.

[4] Z. Yang ; D. Zhang ; X. Sun, X. Ye, 'Adaptive Exponential Sliding Mode Control for a Bearingless Induction Motor Based on a Disturbance Observer', IEEE Access, 2018, vol. 6, pp. 35425 – 35434.

[5] Lascu, C., Boldea, I., Blaabjerg, F.: 'Comparative study of adaptive and inherently sensorless observers for variable speed induction motor drives', IEEE Trans. Ind. Electron., 2006, 53, (1), pp. 57–65.

[6] Vaclavek, P., Blaha, P., 'Lyapunov function based flux and speed observer for AC induction motor sensorless control and parameter estimation', IEEE Trans. Ind. Electron., 2006, 53, (1), pp. 138–145.

[7] Harnefors, L., Hinkkanen, M., 'Complete stability of reduced order and full order observers for IM drives', IEEE Trans. Ind. Electron., 2008, 55, pp. 1319–1329.
[8] H. Wang, X. Ge, Yong-Chao Liu, 'Second-Order Sliding-Mode MRAS Observer-Based Sensorless Vector Control of Linear Induction Motor Drives for Medium-Low Speed Maglev Applications', IEEE Trans. Ind. Electron., 2018, vol. 65, no. 12, pp. 9938 – 9952.
[9] Cirrincione, M., Pucci, M., Cirrincione, G., Capolino, G.A.: 'Sensorless control of induction motors by reduced order observer with MCA-EXIN based adaptive speed estimation', IEEE Trans. Ind. Electron., 2007, 54, pp. 150–166.
[10] Alonge, F., D'Ippolito, F., Giardina, G., Scaffidi, T., 'Design and low cost implementation of an optimally robust reduced order rotor flux observer for induction motor control', IEEE Trans. Ind. Electron., 2007, 54, pp. 3205–3216.
[11] Hinkkanen, M., Harnefors, L., Luomi, J., 'Reduced-order flux observers with stator resistance adaptation for speed sensorless induction motor drives'. IEEE Energy Conversion and Exposition, San Jose, CA, 2009, pp. 155–162.
[12] Montanari, M., Peresada, S.M., Rossi, C., Tilli, A., 'Speed sensorless control of induction motors based on a reduced-order adaptive observer', IEEE Trans. Control Syst. Technol., 2007, 15, pp. 1049–1064.
[13] Utkin, V.I., Guldner, J.G., Shi, J., 'Sliding mode control in electromechanical systems' (Taylor and Francis, New York, 1999, 1st edn).
[14] Yan, Z., Utkin, V.I., 'Sliding mode observers for electric machines – an overview'. Twenty-eighth Annual Conf. on Industrial Electronics Society (IECON '02), Sevilla, Spain, 2002, vol. 3, pp. 1842–1847.
[15] M. Comanescu., 'Single and double compound manifold sliding mode observers for flux and speed estimation of the induction motor drive', IET Electr. Power Appl., 2014, Vol. 8, Iss. 1, pp. 29–38.
[16] L. Zhang, H. Obeid, S. Laghrouche, M. Cirrincione, 'Second Order Sliding Mode Observer of Linear Induction Motor', IET Electric Power Applications, 2019, vol. 13, no. 1, pp. 38 – 47.
[17] Lascu, C., Boldea, I., Blaabjerg, F., 'A class of speed-sensorless sliding-mode observers for high-performance induction motor drives', IEEE Trans. Ind. Electron., 2009, 56, (9), pp. 3394–3403.
[18] Li, J., Xu, L., Zhang, Z.: 'An adaptive sliding mode observer for induction motor sensorless speed control', IEEE Trans. Ind. Appl., 2005, 41, pp. 1039–1046.
[19] M. S. Zaky, M. K. Metwaly, H. Z. Azazi, S. A. Deraz, 'A New Adaptive SMO for Speed Estimation of Sensorless Induction Motor Drives at Zero and Very Low Frequencies', IEEE Trans. Ind. Electron., 2018, vol. 65, no. 9, pp. 6901 – 6911.
[20] Derdiyok, A., Yan, Z., Guven, M., Utkin, V.I., 'A sliding mode speed and rotor time constant observer for induction machines', The 27th Annual Conf. on IEEE Industrial Electronics Society, 2001, pp. 1400–1404.
[21] Rehman, H., Derdiyok, A., Guven, M.K., Xu, L., 'A new current model flux observer for wide speed range sensorless control of an induction machine', IEEE Trans. Power Electron., 2002, 7, (6), pp. 1041–1048.
[22] Zhang, Z., Xu, H., Xu, L., Heilman, L.E., 'Sensorless direct field-oriented control of three-phase induction motors based on sliding mode for washing machine drive applications', IEEE Trans. Ind. Appl., 2006, 42, (3), pp. 694–701.
[23] M. Comanescu 'Design and Implementation of a Highly Robust Sensorless Sliding Mode Observer for the Flux Magnitude of the Induction Motor', IEEE Trans. on Energy Conversion, 2016, vol. 31, no. 2, pp. 649 – 657.
[24] B. Wang, C. Luo, Y. Yu, G. Wang, D. Xu, "Anti-Disturbance Speed Control for Induction Machine Drives Using High-Order Fast Terminal Sliding-Mode Load Torque Observer", IEEE Trans. Power Electron., 2018, vol. 33, no. 9, pp. 7927 - 7937.
[25] Rao, S., Buss, M., Utkin, V.I.: 'Simultaneous state and parameter estimation in induction motors using first and second order sliding modes', IEEE Trans. Ind. Electron., 2009, 56, (9), pp. 3369–3376.
[26] Korlinchak, C., Comanescu, M.: 'Robust sensorless sliding mode flux observer with speed estimate for induction motor drives', Electr. Power Compon. Syst. J., 2012, 40, (9), pp. 1030–1049.
[27] Comanescu, M.: 'A family of sensorless observers with speed estimate for rotor position estimation of im and pmsm drives'. Industrial Electronics Conf. (IECON 2012), Montreal, Canada, October 2012, pp. 3670–3675.
[28] Korlinchak, C., Comanescu, M.: 'Sensorless field orientation of an induction motor drive using a time-varying observer', IET Electr. Power Appl., 2011, 6, pp. 1–9.
[29] Proca, A.B., Keyhani, A.: 'Sliding-mode flux observer with online rotor parameter estimation for induction motors', IEEE Trans. Ind. Electron., 2007, 54, (2), pp. 716–723.
[30] Comanescu, M., Utkin, V.I.: 'A sliding mode adaptive MRAS speed estimator for induction motors'. IEEE Int. Symp. on Industrial Electronics, 2008, pp. 634–638.
[31] H. Wang ; Yong-chao Liu ; Xinglai Ge, "Sliding-mode observer-based speed-sensorless vector control of linear induction motor with a parallel secondary resistance online identification", IET Electric Power Applications, 2018, vol. 12, no. 8, pp. 1215 – 1224.
[32] M. H. Holakooie, M. Ojaghi, A. Taheri, "Modified DTC of a Six-Phase Induction Motor With a Second-Order Sliding-Mode MRAS-Based Speed Estimator", IEEE Trans. Power Electron., 2018, vol. 34, no. 1, pp. 600 – 611.
[33] Eberhart RC, Shi Y. 'Particle swarm optimization: developments, applications and resources', In: Proceedings of the 2001 congress on evolutionary computation, vol. 1; 27–30 May, 2001. p. 81–6.
[34] M. S. Zaky, M. K. Metwaly, H. Z. Azazi, S. A. Deraz, "A New Adaptive SMO for Speed Estimation of Sensorless Induction Motor Drives at Zero and Very Low Frequencies", IEEE Trans. Ind. Electron., 2018, vol. 65, no. 9, pp. 6901 – 6911.
[35] W. C. A. Pereira, C. M. R. Oliveira, M. P. Santana, T. E. P. Almeida, A. G. Castro, G. T. Paula, M. L. Aguiar, "Improved Sensorless Vector Control of Induction Motor Using Sliding Mode Observer", IEEE LATIN AMERICA TRANSACTIONS, 2016, vol. 14, no. 7, pp. 3110 – 3116.
[36] P. Vas, "Sensorless Vector and Direct Torque Control", Oxford University Press, 1998.